Observation of the Loop-Top Source of the 1998 April 23 flare

Jun Sato and Yoichiro Hanaoka

Nobeyama Radio Observatory, NAOJ Nobeyama, Minamimaki, Minamisaku, 384-1305, Japan
E-mail(JS): sato@nro.nao.ac.jp

Abstract

We analyzed the loop-top source of an X 1.2 flare on 1998 April 23, based on the hard X-ray and the microwave observations. This flare is an impulsive one which is accompanied by a remarkable coronal eruptive event. Since this flare occurred slightly behind the solar limb, the footpoint emission, which is usually dominant, was blocked by the limb. Therefore, only the source located at the loop-top region is well observed. The hard X-ray emission of the loop-top source is revealed to come from both the nonthermal electrons and the thermal plasma. The power-law index of the nonthermal electrons, δ, derived from the hard X-ray observation is about 2.9 on the assumption of the thin-target model. This is consistent with the index of 2.5–3 derived from the dual-frequency observation in microwaves. On the other hand, the temperature of the thermal plasma is derived to be about 33 MK. The thermal and the nonthermal components show complicated spatial structures, and the source position of the nonthermal component does not show a good coincidence to that of the thermal component.

Key words: Sun: flare — Sun: X-rays — Sun: microwaves

1. Introduction

The finding of the high-energy hard X-ray source located above the soft X-ray loop, namely the loop-top impulsive source or so-called 'the Masuda source' (Masuda et al. 1994), is one of the most important scientific results obtained with the Hard X-ray Telescope (HXT; Kosugi et al. 1991) on board the *Yohkoh* satellite. Furthermore, Shibata et al. (1995) pointed out that most of the flares studied by Masuda et al. (1994) were accompanied by coronal eruptive events. These observations suggest that the energy release of the flares induced by coronal eruptions occurs above the top of the flare loops. Therefore, in order to understand the mechanism and the site of the electron acceleration of the flares accompanied by coronal eruptions, it is extremely important to study the characteristics of the loop-top impulsive source of the flares. Although various studies from both the observational and the theoretical viewpoints have been done so far (e.g., Masuda et al. 1994, Wheatland, Melrose 1994, Alexander, Metcalf 1997), the characteristics of the loop-top source is not very clear. The most basic property of the loop-top source, whether the emission has a thermal origin or a nonthermal one, is still controversial. This is due to the following reasons. (1) Precise measurements of the hard X-ray brightness of the relatively weak loop-top source is difficult in the presence of strong hard X-ray sources at the footpoints. (2) It was difficult to obtain hard X-ray images with both a high-time resolution and a high dynamic range, because the flares studied by Masuda et al. (1994), which occurred near the limb, are at most M-class flares. (3) It was very difficult to synthesize hard X-ray images of large-sized structures before the improvement of the HXT imaging (Sato J. et al. 1999). (4) There was no simultaneous observation of the loop-top source in hard X-rays and radio frequencies. The radio observations of flares give information of the higher-energy electrons than that of the hard X-ray emitting electrons.

To clarify the characteristics of the loop-top sources, we analyze two intense limb flares in region NOAA 8210. This region was observed from April in 1998 through May and was a flare productive region. The analyzed flares are an X1.2 flare on April 23 and an M7.7 flare on May 9. In these flares, coronal eruptive events were also observed with the Soft X-ray Telescope (SXT; Tsuneta et al. 1991) on board *Yohkoh* before the impulsive phase of the flares. Therefore both of them are the impulsive flares induced by the coronal eruptive events. Both the flares occurred when the active region was slightly behind the limb; the longitude of the active region at the April 23 flare is E103, and that at the May 9 flare is W101. The position of the limb is 17,000 km high above the active region in the case of the April 23 flare. Therefore, intense emission from the footpoints is occulted by the solar limb, and the observed images are considered to be purely the images of the loop-top sources. These flares were well observed with

the HXT and the Nobeyama Radioheliograph (NoRH; Nakajima et al. 1994), simultaneously. Although the hard X-rays and the microwaves come from the loop-top sources only, they are strong enough to study the characteristics of the loop-top source with a higher time-resolution and a higher quality of images than the previous observations. Consequently, the analysis of these flares gives unique information about the emission from the loop-top region of the flares induced by coronal eruptions, though the information on the footpoint sources are lacking.

The two flares have various common characteristics as described above. Therefore, in the following sections, we only present the results of the analysis of the larger one, the 1998 April 23 flare.

2. Overview of the 1998 April 23 Flare

The brightness variations of the X1.2 flare on 1998 April 23 in microwaves observed with the NoRH (17 GHz and 34 GHz) and in hard X-rays observed with the HXT (L-band:14–23 keV, M1:23–33, M2:33–53, H:53–93) are shown in figure 1. Figure 2 shows the images of the 1998 April 23 flare observed with the SXT, the HXT (L/M2-bands) and the NoRH (17 GHz) from the impulsive phase through the decay phase. As mentioned in section 1, since the active region is behind the limb, the bright structure seen in figure 2 is located at the loop-top.

Before the flare onset, at 05:30 UT, a coronal eruption took place. The eruption was observed with the SXT, and also with the LASCO of SoHO later on. The impulsive brightening of the flare started at 05:36, and the intense hard X-ray and microwave emission was simultaneously observed with the HXT and the NoRH. At 05:36, the ascending speed of the erupting loop, of which height is about 100,000 km, is about 350 km s^{-1}. The soft X-ray images in figure 2 show an elongated bright structure above the limb from the impulsive through the decay phases. This structure is the ridge of a soft X-ray arcade, and its apparently ascending motion is observed in the decay phase. The soft X-ray arcade brightening lasts for several hours, while the duration of the impulsive brightening in hard X-rays and microwaves is about ten minutes.

3. Spectral Characteristics of the Loop-Top Source

In this section, the time variations and the spectral characteristics of the 1998 April 23 flare are discussed. As shown in figure 1, the HXT recorded high energy photons, and the time profiles both in microwaves and hard X-rays of the higher energy bands (M2/H) show similar spike structures, although their duration and detailed structures are different from each other.

The measured microwave brightness at 17 GHz and 34 GHz of this flare is extremely large, and such an intense brightening is due to the gyrosynchrotron emission from the nonthermal high-energy electrons. This is the evidence of the existence of the high-energy electrons in the loop-top region. The ratio of the brightness at 17 GHz to that at 34 GHz is related to the index of the power-law spectrum of the high-energy electrons. The spectral index δ derived from the intensity ratio, which is about 2, is 2.5–3. Therefore, the spectrum is harder than the typical values ($\sim$4) observed in the footpoint regions. In addition, the intensity ratio does not change so much throughout the impulsive phase.

While the radio observations show the behavior of high-energy electrons of which energy is probably the order of 1 MeV, the observations with the HXT show the behavior of the electrons up to about 200 keV. In this energy range, generally the hard X-ray emission comes from both the thermal plasma and the nonthermal electrons. Figure 1 shows much different time profiles in the four energy bands of the HXT. While the H- and M2-bands shows impulsive nature and a similar duration to that of the microwaves, the L-band shows a gradual time variation. Probably the loop-top hard X-ray emission includes both the thermal and the nonthermal components. Then, we try to divide the observed hard X-ray counts into the thermal component and the nonthermal (power-law) one. We assume a simple 'two-component model', consisting of a thermal component with a single temperature and a nonthermal component with a single power-law spectrum. Since there are four count rates, we can derive a unique solution of the parameter set of the two components, namely temperature and amount of the thermal plasma, and index and amount of the power-law electrons. The results are shown in figures 1b–e. The gray and black areas show the estimated counts of the thermal and the nonthermal components, respectively. The calculation cannot be carried out when the H-band shows no substantial count rate. Excepting the first spike at 05:37 when the two-component model fails to give a meaningful solution, we successfully calculated the parameter sets for the two components for most of the time range. As shown in these figures, the thermal component is dominant in the L- and the M1-bands, while the nonthermal component is dominant in the M2- and the H-bands. As mentioned in section 1, the thermal/nonthermal issue of the loop-top source is still controversial, but our result shows that the loop-top hard X-ray emission is a mixture of the thermal and the nonthermal components. Near the peak time, temperature of the thermal component is calculated

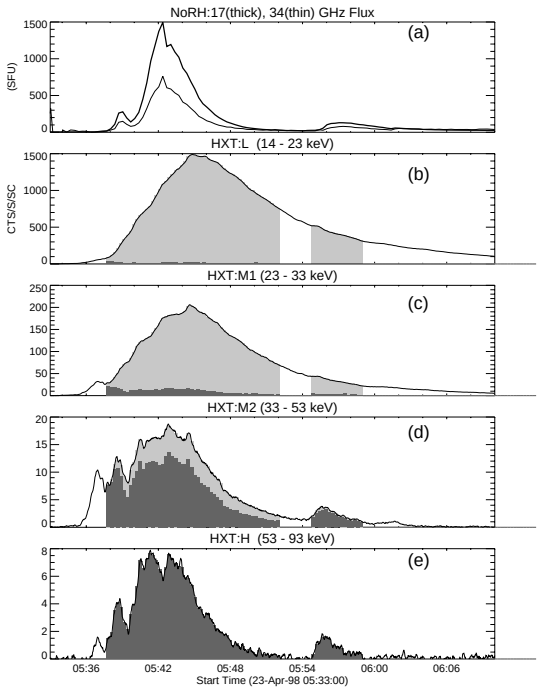

Fig. 1.. (a) Microwave (17GHz in the thick line and 34 GHz in the thin line) flux variations measured with the NoRH. (b–e) Hard X-ray intensity variations of the four energy bands of the HXT (solid lines). Gray areas show the calculated contributions from the thermal component, which assumed to have a single temperature. Black areas show the calculated contributions from the nonthermal component on the assumption of a single power-law spectrum.

to be about 33 MK, and the power-law index of the nonthermal hard X-rays, γ, is about 3.4. On the assumption of the thin target model, the power-law index of the nonthermal electrons, δ, is estimated to be 2.9, based on the relation that $\gamma = \delta + 0.5$. The indices of the nonthermal electrons derived from the microwave observation and the hard X-ray one are consistent. Although these results are mainly derived from the intensity time profiles without considering spatial structure, it is plausible that the high-energy hard X-ray source observed in the loop-top region is explained by the thin target model, and that the electrons have a hard spectrum.

4. Spatial Characteristics of the Loop-Top Source

Next, we discuss the spatial structures of the hard X-ray and the microwave sources. Figure 2 shows the images of the 1998 Apr 23 flare observed with the SXT, the HXT (L/M2-bands) and the NoRH (17 GHz) from the impulsive phase through the decay phase. As shown in this figure, with the progress of the flare, the L-band source, which corresponds to the thermal component, moves northward along the top of the soft X-ray arcade structure. In the decay phase, the thermal source increases its height. Similar images to the L-band ones are also obtained in the M1-band (not presented in this paper) as expected from the same thermal plasma.

On the other hand, the M2-band images show more complicated spatial structures as expected from the fact that the counts of the M2-band consist of a mixture of thermal/nonthermal components as shown in figure 1d. At the beginning, the hard X-ray source is adjacent to the L-band source in the southern region. Near the peak time and in the decay phase, two bright sources are observed in the southern and the northern regions. The northern source is located at the bright core observed in the L-band. The brightness of this source is explained by the emission from the thermal plasma, of which the temperature and the emission measure are estimated from the count ratio between the L-band and the M1-band. This means that the northern source is a purely thermal source. On the other hand, the southern source and a diffuse structure extending above the two sources show very weak emission in the L-band, and therefore, this source is the nonthermal source. In the microwave images, as a whole, the bright region shifts from the south to the north during the flare, In addition, the source size seems to be increasing near the peak time. This increase of the size may be related to the faint structure observed in hard X-rays. However, in

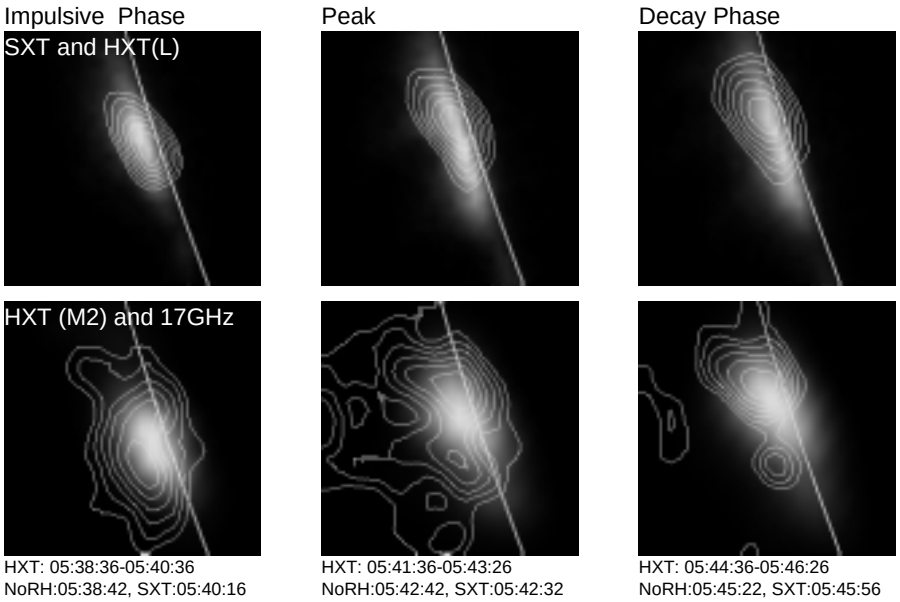

Fig. 2.. Soft X-ray images taken with the SXT with the Be filter, hard X-ray images taken with the HXT, and microwave images at 17GHz taken with the NoRH, from the impulsive phase through the decay phase. Top panels show the soft X-ray images (gray scale) and the hard X-ray images of the HXT L-band (contours). Bottom panels show 17 GHz images (gray scale) and hard X-ray images of the HXT M2-band (contour). The field of view of each map covers 79×79 arcsec. The brightness scale of each map is normalized within the map. Contour levels are 70.7, 50.0, 35.4, 25.0, 17.6, 12.5 % of the maximum brightness.

detail, the spatial structures of the nonthermal components observed in both microwaves and hard X-rays do not necessarily agree with each other, e.g., the hard X-ray source is located above the microwave source. Further study of the spatial structures is needed.

In this paper, we show that the analysis of the 1998 April 23 flare, which occurred slightly behind the limb, reveals the various characteristics of the loop-top impulsive sources. Although the footpoint sources are not observed, such analyses have the unique capability to study the the nature of the loop-top sources. This paper is just a brief report of the analysis of the 1998 April 23 flare, and the detailed description of the analysis of this flare as well as the 1998 May 9 flare will be given in the forthcoming paper.

References

Alexander D., Metcalf T. R. 1997, ApJ,**489**, 442
Kosugi T., Makishima K., Murakami T., Sakao T., Dotani T. et al. 1991, Solar Phys. 136, 17
Masuda S., Kosugi T., Hara H., Tsuneta S., and Ogawara Y. 1994, Nature 371, 495
Nakajima H., Nishio M., Enome S., Shibasaki K., Takano T. et al. 1994, Proc. IEEE 82, 705
Sato J., Kosugi T., and Makishima K. 1999, PASJ, in press
Shibata K., Nasuda S. et al. 1995, ApJ Lett., 451, L83
Tsuneta S., Acton L., Bruner M., Lemen J., Brown W. et al. 1991, Solar Phys. 136, 37
Wheatland M.S., Melrose D.B. 1994, Solar Phys. 185, 283